

# Policies affecting the spread of COVID-19

Ethan Tregidga 30731003<sup>1</sup>\*

<sup>1</sup>*Faculty of Engineering and Physical Sciences, University of Southampton, Southampton SO17 1BJ, UK*

23 October 2022

## ABSTRACT

This report aims to understand the effect of UK policies on reducing the spread of COVID-19. A program was written that broke the problem into three scales and combined random walk and Monte Carlo simulations to model the propagation of COVID-19. The first is the spread of COVID-19 between people in a building. The second is to scale the problem up to the size of a large city by simulating many individual buildings. Finally, the model simulates the evolution over time. The central policies considered were testing, vaccinations, social distancing and lockdowns. Each policy affected the spread of COVID-19 in different ways, with vaccinations and social distancing having the most significant impacts due to a high level of protection from vaccinations, the quick implementation of social distancing, and the sensitivity of the direct spread of COVID-19 between people.

**Key words:** COVID-19 – Monte Carlo – Random walk – Pandemic – Viruses

## 1 INTRODUCTION

This report aims to model the dynamics of the spread of a disease using a Monte Carlo simulation. COVID-19 will be used to model the effects of different policies to reduce or prevent outbreaks of new diseases.

First reported in Wuhan in China at the end of 2019, COVID-19 was quickly classified as a pandemic in March 2020 by the World Health Organisation (WHO) (Gautret et al. 2020).

COVID-19 is highly infectious and spreads mainly via respiratory droplets. One of the difficulties in containing the spread of COVID-19 is that it can be both symptomatic and asymptomatic; therefore, a portion of infected people will be unaware that they are infected.

As the virus spread through populations, governments implemented different policies with varying levels of restrictions to try and reduce the spread, with each country experiencing various successes or failures. Some standard methods used were increased hygiene, social distancing, face masks, track and trace, testing facilities and self-testing, lockdowns, self-isolation, vaccinations and stricter border control.

Out of these methods, the model will simulate social distancing, self-testing, lockdowns, self-isolation, and vaccinations to determine the effectiveness in reducing the spread of COVID-19.

## 2 METHOD

The program was written in three key stages. The first stage is the movement of people around a building. This is done by defining a maximum step size based on the maximum speed that someone can move in a busy building and using random numbers to determine each

person's path. A simplistic approach was taken where each person represents a point and can choose a random direction to move in with a step size that can vary between zero and the maximum value in a uniform distribution. There is no awareness between different people, and the only constraint is that a person cannot leave the building. The people in the building will move for several steps before the simulation of that building stops. This number is constant throughout the simulation for all buildings. The probability of infection can be calculated by the distance between an infected person and an uninfected person combined with a probability distribution.

The following scale of creating a city is done by a collection of buildings that can each contain several people. As each building has a limited capacity, there is a limited number of people who can be active each day. As fewer people are doing a random walk than total people, it would correspond to not everyone going to a public place at a time.

The final stage of the problem is to track the spread of COVID-19 over time. Each run of building simulations can represent one day. The stage of infection is broken up into three types: incubating, contagious and recovered, with the progress advancing each day.

### 2.1 Setting up the environment

The shortest scale can be modelled by defining two properties for each building, its area and capacity. A paper by Borchert (1998) looked at the average size of buildings per population size and found the average area per store in a city was  $164 \text{ m}^2$  and a density of  $0.86 \text{ people/m}^2$ . As seen in figure 1, each building was drawn from a Gaussian probability distribution with upper and lower limits to the size and density. The area had limits of  $20 \text{ m}^2$  to  $2000 \text{ m}^2$  and  $0.02 \text{ people/m}^2$  to  $2 \text{ people/m}^2$  for the density as found in an engineering report (ToolBox 2003).

In order to determine the maximum walking speed,  $u_j$ , in each

\* E-mail: etlg19@soton.ac.uk

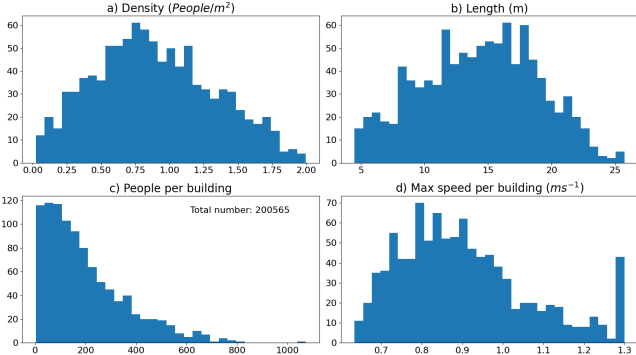


**Figure 1.** Distributions of the building properties that make up the simulation. A sample of 1000 buildings with a total capacity of 200,565 people. The spike in seen in (d) at  $1.3 \text{ ms}^{-1}$  is due to the upper limit for the average walking speed.

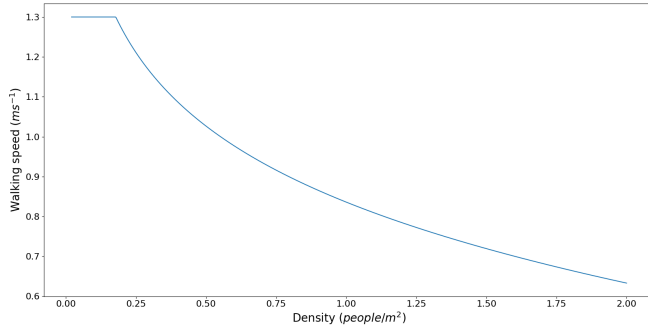


**Figure 2.** A plot of equation 1 giving the relationship between the maximum walking speed of an individual and the density of a crowded room. In this report, the maximum walking speed was taken to be a constant of  $1.3 \text{ ms}^{-1}$  with densities up to  $0.18 \text{ people/m}^2$  being equivalent to free motion.

building, as seen in figure 2, two factors need to be considered. First, the average free walking speed,  $u_m$ , is the speed of a person who is not restricted by the presence of surrounding people with density,  $\rho$ , as calculated above, which applies a resistance to motion.

In a paper by Chandra & Bharti (2013), the average free walking speed was found to be around  $u_m = 1.3 \text{ ms}^{-1}$  so this will be the value used.

A paper by Fang et al. (2003), they derived equation 1 to predict the walking speed of a person in a crowd where  $\rho_{1c} = 0.89$  and  $\rho_{2c} = 1.33$  are the critical front-back and lateral densities respectively for a person to travel freely,  $\rho_{1m} = 3$  and  $\rho_{2m} = 2$  are the maximum densities for over-crowding and it is assumed the front-back and lateral densities are equal with the product of them equal to the area density,  $\rho_1 = \rho_2 = \sqrt{\rho}$ , combined with a transformation,

$$\rho_1^* = (\rho_{1c} + \rho_{1m})/2, \quad \rho_2^* = (\rho_{2c} + \rho_{2m})/2$$

and the values for  $\alpha$ ,  $\beta$  and  $\gamma$  are given by the curve fitted values for data from Predtechenskii (1978) with a lateral width of 0.9 giving  $\alpha = 0.24$ ,  $\beta = 0.025$  and  $\gamma = 0.27$ .

$$u_j(\rho_1, \rho_2) = u_m \left( \alpha \frac{\ln(\rho_{1m}\rho_2^*/\rho)}{\ln(\rho_{1m}/\rho_{1c})} + \beta \frac{\rho_1^*\rho_{2m} - \rho}{\rho_1^*(\rho_{2m} - \rho_{2c})} + \gamma \right) \quad (1)$$

## 2.2 Spread of COVID-19 between people

COVID-19 can be introduced into the problem by defining three types of people: contagious people who can spread COVID-19, infected people who are not contagious as they are still in the incubation phase, and uninfected people. Each person is randomly assigned to a building until each building has reached its maximum capacity. Suppose there are not enough people to fill every building, which could be due to people in isolation. In that case, the densities of buildings are scaled by the difference in people and total capacity. Each person can only visit up to one building per day to simplify the model.

The movement of people in a building is then decided by a random number generator which decides the direction that a person will walk in and the distance travelled. Each step taken is treated as one second; therefore, the maximum speeds calculated in section 2.1 would correspond to the maximum distance that a person can travel per step. A uniform distribution was chosen for both the direction and the step size. This distribution allows freedom of movement in all directions and simulates stationary or idle movement with an equal probability for small step sizes.

The probability that an uninfected person gets COVID-19 from an infected person can be calculated from a distance between each infected person and the probability distribution from equation 2

Equation 2, was derived in a paper by Bale et al. (2021) where they analysed the risk of infection by modelling droplet dispersion. The model assumes a Poisson infection probability where  $N_0$  is the average number of virions to infect someone,  $N$  is the current number inhaled, and  $\alpha$  will correspond to the efficacy of protection for a person,  $\eta$ , multiplied with the transmissibility factor,  $\tau$ , of the variant giving  $\alpha = \tau(1 - \eta)$ . This value will equal one for the ancestral strain and with no protection. However, this does not consider seasonal variability in the spread of COVID-19.

In the paper,  $N_0 = 900$  will be used in this paper. The value for  $N$  is calculated using the second part of equation 2 where  $B$  is the breathing rate taken to be  $0.54 \text{ m}^3 \text{ hr}^{-1}$ ,  $\lambda_v$  is the number of virions per volume of droplets taken to be  $7 \times 10^{12} \text{ m}^{-3}$  and the volume inhaled,  $v_B$  is assumed to be a  $0.1 \text{ m} \times 0.1 \text{ m} \times 0.15 \text{ m}$  cuboid. For the last two variables, the time taken,  $T$ , will be adjusted in section 2.3 and the volume of the droplets over distance,  $v_d^0$  will be approximated by equation 3, where  $d$  is the separation distance, to achieve a similar probability distribution used in the paper.

However, this model only considers the direct infection from person to person via droplets and not from alternate ways of contracting the virus, such as via contact with surfaces or inhalation of viral particles that stay suspended in the air after the infected person has left the area.

$$P = 1 - e^{-\alpha \frac{N}{N_0}}, \quad N = \frac{B\lambda_v v_d^0 T}{v_B} \quad (2)$$

$$\bar{v}_d^0(d) = \left( 0.8 \times 10^{12} d^2 + 0.1 \times 10^{12} d + 0.45 \times 10^{12} \right)^{-1} \quad (3)$$

## 2.3 Evolution of COVID-19 and policies to reduce the spread

The model aims to replicate the spread of COVID-19 following data primarily from the UK; therefore, the policy timelines will replicate when the UK implemented them relative to when control over the spread of COVID-19 was lost. For simplicity, the date was the 1st of January 2020, which corresponds to day 1 in this report. The spread

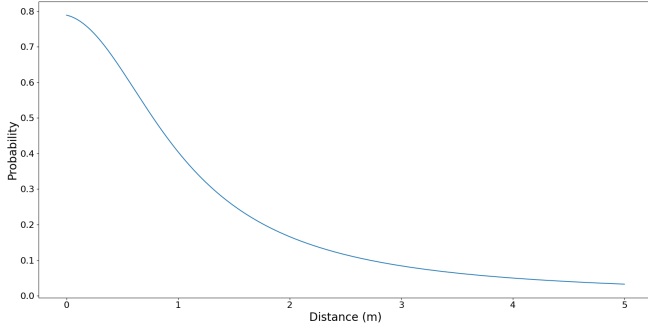


**Figure 3.** Probability of COVID-19 infection over distance given by equation 2 for a time of 15 minutes.

of COVID-19 over time can be simulated by following a schedule for each day as follows:

- (i) First, calculate the number of people recovered from COVID-19.
- (ii) Vaccinate several people if vaccinations are in effect.
- (iii) Calculate probabilities of a positive test for some infected people who then go into isolation if testing is in action.
- (iv) Finally, simulate a random walk to calculate new infections.

Each individual is tracked so that properties like their natural immunity and vaccination status are kept constant. A separate array will keep track of everyone infected to monitor the current stage of infection.

In order to simulate the effects of policies in reducing the spread, the model will have to run for several simulated days over a large population. A population size of 250,000 people was used to balance accuracy and computation speed. However, only 200,000 people would visit a building per day to simulate a portion of people who do not leave the house for a day. Using the average person density distribution found in section 2.1, this required 1,000 buildings for a total capacity of 200,565 people. Each policy will be run three times to obtain an average and standard error to reduce the noise due to random sampling and get estimates on the significance of the differences between models.

The following subsections will cover the different stages of the day and how they are calculated in reverse chronological order, starting with the calculation of infections.

### 2.3.1 Infections

After running the random walk simulation and the number of new infections found, the infection's life cycle can be calculated for each person. The cycle will follow an incubation phase followed by the contagious phase. The infection can be either symptomatic or asymptomatic. First, the type of infection is determined by the probability of the number of asymptomatic people compared to the symptomatic number. The chosen probability came from a study by [Alene et al. \(2021\)](#) where they found that roughly one-quarter of COVID-19 cases are asymptomatic.

For the duration of the different phases of infection, a log-normal distribution was found to be the best fit for all phases in two papers: [McAloon et al. \(2020\)](#), who reviewed incubation periods, and [Byrne et al. \(2020\)](#), who reviewed symptomatic and asymptomatic periods. The log-normal distribution takes two parameters,  $\mu$  and  $\sigma$ . The distributions used by this paper can be seen in figure 4. The parameters used for the incubation phase are  $\mu_{inc} = 1.63$  and  $\sigma_{inc} = 0.5$

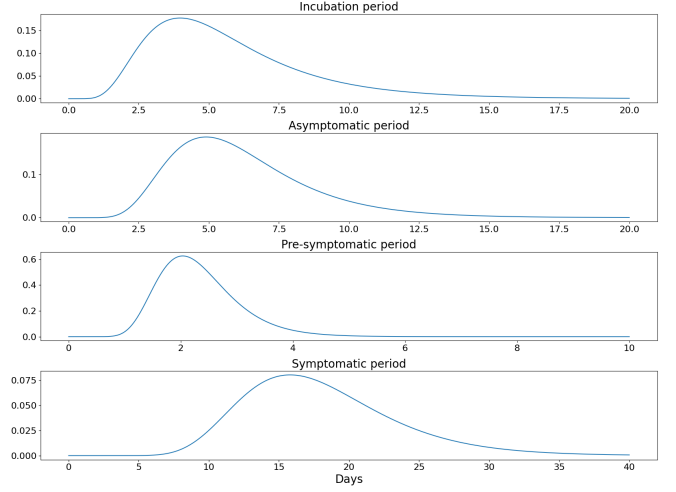


**Figure 4.** Log-normal distributions for the period of different phases of infection.

for the incubation phase. This distribution will be the same for asymptomatic and symptomatic cases. For the asymptomatic duration,  $\mu_{asym} = 1.75$  and  $\sigma_{asym} = 0.4$ . Finally, the symptomatic duration is split into the pre-symptomatic and symptomatic phases. The pre-symptomatic phase is where the person is now infectious; however, symptoms have not developed yet. The parameters used are  $\mu_{pre} = 0.8$ ,  $\sigma_{pre} = 0.4$ ,  $\mu_{sym} = 2.85$  and  $\sigma_{sym} = 0.3$  for the  $\mu$  and  $\sigma$  for pre-symptomatic and symptomatic respectively. These values were chosen to match the distributions given in the paper.

### 2.3.2 Mutations

As viruses replicate, they undergo several mutations, many of which do not affect the properties of the virus; however, sometimes, it can result in favourable mutations for the virus, such as increased transmissibility. Due to the rapid replication rate of viruses, these mutations occur much more often than in animals, so new variants of the virus can form over a short time.

COVID-19 has undergone several significant mutations resulting in the creation of new variants. This report will focus on the main strains that affect transmissibility, including the original strain, the Alpha variant, the Delta variant, and the Omicron variant; however, the latter will not be covered as this report focuses on the beginning of the pandemic.

As mentioned in section 2.2, the  $\alpha$  value is proportional to the transmissibility,  $\tau$ , of COVID-19, which is initially set to one for the ancestral strain.

In the paper which proposed the equation, the Alpha variant had  $\tau = 1.29$ . However, in order to replicate a reproductive value,  $R_0$  between 4-5 as found by [Hendaus & Jomha \(2021\)](#),  $\tau$  was set to 2. The method to find  $\tau$  will be covered in section 2.4. The method used to combine transmissibility and efficacy in equation 2 and the approximation of equation 3 is likely responsible for this difference.

The Alpha strain originated in the UK; therefore, the start is not precisely known; however, it is believed to have started in late September to early October 2020, as found in a paper by [Heath et al. \(2021\)](#). Therefore, the variant will begin on day 270 in the model with the approximation that  $\tau$  will increase linearly over 60 days to simulate the new variant becoming the dominant strain. Sixty days were chosen

as this was how long it took for the Delta variant to become dominant as found in [Pouwels et al. \(2021\)](#).

The same process can be done for the Delta variant and a value of  $\tau = 3$  was chosen which gave  $R_0 =$  which is within uncertainty of the target of  $R_0 = 5.08$  as found in a paper by [Thye et al. \(2021\)](#). The start date for the new variant will be in May 2021, which corresponds to day 480 of the model as reported by [Pouwels et al. \(2021\)](#). A linear increase is again used between the Alpha variant and the Delta variant over 60 days.

### 2.3.3 Testing

Testing can be broken down into two parts. The first is regular testing, and the second is testing when someone starts having symptoms. However, this is a rather simplistic approximation as it does not consider the current number of cases and if this would influence the testing rate or the difference in testing if someone came in contact with an infected person.

After someone tests positive, they will go into isolation where they will not participate in the random walk and therefore will not spread the virus until they are no longer contagious.

However, this does not account for people going into isolation without any positive test, especially early on before mass testing when the government advised people to isolate if they had symptoms or were in contact with someone who recently tested positive. It also does not simulate people leaving isolation too early if they either no longer have symptoms but are still contagious or if their contagious period was longer than the government-mandated time for isolation. This model also assumes that everyone who tests positive will isolate; however, humans are not always rational; therefore, some people might ignore test results or may have incorrectly taken a test.

The total number of people taking regular tests can be estimated from the number reported by the UK government website ([UK government 2022a](#)) as well as an estimate of the number of people who do not report their tests as found in the UK government census report ([UK government 2022b](#)). From the government data, the number of reported cases is around 1.5%. However, this report assumes that the number of reported cases are from unique individuals and not repeated tests.

The number of unreported cases is estimated from people's attitude in reporting their results. However, this does not consider any bias between positive or negative results, and the survey only asked people who recently came into contact with someone who tested positive. In the report, 35% stated that they never intended to report their results and 31% stated they consistently reported them. The remaining 34% was a mix of sometimes and often; therefore, an approximation of a 50% report rate was taken for these people combining to produce an overall test report rate of 50% leading to the number of tests taken per day being around 3%.

People who are showing signs of symptoms are assigned a higher test rate as it was found that 48% of people took a COVID-19 test because they showed symptoms ([UK government 2020](#)). Therefore, the test rate was split in half assigning 1.5% to symptomatic people and 1.5% to everyone else.

To model the number of tests taken over time, an initial delay of 120 days where no tests were taken, and then a linear build-up over 365 days to the maximum value of 3% of tests taken. The linear model was used to replicate the data collected by the government on the reported test rates.

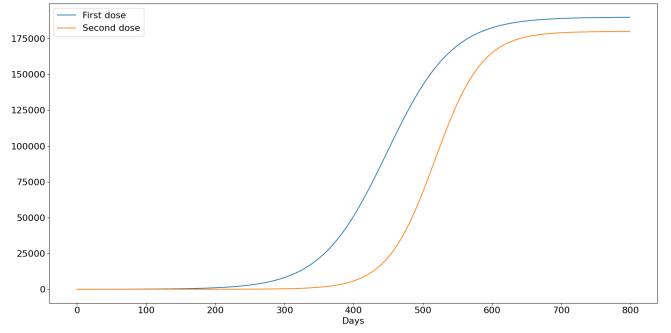


**Figure 5.** The cumulative number of vaccinated people using equation 4. The fitted parameters were  $N_m = 190,000$ ,  $m = 0.021$  and  $c = 9.4$  for the first vaccination number and  $N_m = 180,000$ ,  $m = 0.029$  and  $c = 15$  for the second dose.

### 2.3.4 Vaccinations

Due to COVID-19 reaching pandemic levels and becoming a world health concern while also being similar to the previous SARS-Coronavirus, vaccine development happened in record time, resulting in their roll-out in the UK in December 2020. Another advantage of vaccines is that they have very high efficacies, around 82% after the first dose and 95% after the second, as reported in a paper by [Polack et al. \(2020\)](#).

However, several simplifications were made, such as no change in asymptomatic chance due to increased immunity, the vaccination's immediate effect, and no fall-off of vaccine efficacy over time.

The rate of vaccinations in the UK can be calculated from the cumulative vaccination numbers on the government website, and a sigmoid function, equation 4, can be fitted for both doses as seen in figure 5.  $N(t)$  is the current number of people with a vaccination,  $N_m$  is the maximum number of people vaccinated,  $m$  and  $c$  are parameters to control the shape, and  $t$  is the time in days. One approximation is that the vaccine efficacy does not change over time or with new strains.

$$N(t) = \frac{N_m}{1 + \exp(-mt + c)} \quad (4)$$

### 2.3.5 Social distancing

Social distancing was a measure implemented to reduce the spread of COVID-19 by increasing the distance between people to reduce the probability of infection. A commonly used number is a separation of  $2\text{ m}$  as found in the UK government report ([UK government 2021](#)) which started in March 2020. Due to the nature of random walk, there is no active measure to maintain a  $2\text{ m}$  distance between people; however, the density of each building can be reduced to allow a  $2 \times 2\text{ m}^2$  area per person, which will on average introduce the  $2\text{ m}$  social distancing. The start date for this is from day 60. The new distributions for buildings after social distancing are seen in figure 6. The average density is now  $0.25\text{ people/m}^2$ ; however, there are buildings with larger densities which would correspond to some cases where social distancing is not possible such as in tight spaces or when people break these rules. Another approximation is that this social distancing will be enforced throughout COVID-19 after its initial implementation; however, this varies in government guidelines and public attitude.

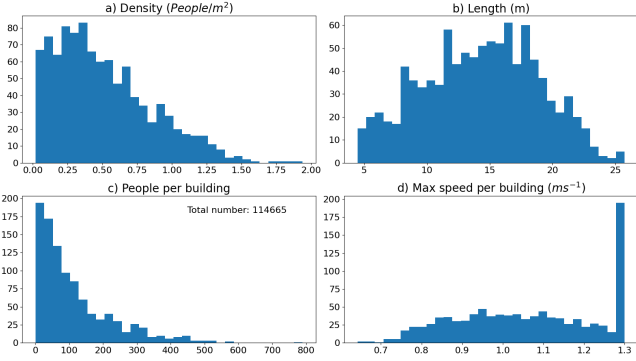


**Figure 6.** Reduced average density of people in a building to simulate social distancing. An average of  $0.25 \text{ people/m}^2$  was chosen which would correspond to a  $2 \times 2 \text{ m}^2$  area per person. The peak in (d) is larger than without social distancing due to the greater space per person and therefore less restricted flow of people.

### 2.3.6 Lockdowns

An alternate measure to social distancing is enforcing lockdowns. A lockdown is where only essential businesses are allowed to remain open. In the UK, there were three national lockdowns which can be found on the UK parliament website (Parliament 2021), the first was from late March to mid-June 2020, the second was from early November to early December, and the last was from early January to early March. However, the periods of national lockdowns vary in what businesses are allowed to be open. Even after each lockdown, there were varying levels of restrictions, such as the several tiers first announced in mid-October 2020. In a report by the Office for National Statistics (for National Statistics 2021), they analysed the effect of lockdown on the number of businesses that had to close. When accounting for all industries, they found 24%, 11% and 12% of all businesses closed in the first lockdown, second and third lockdown, respectively.

Lockdowns can be simulated by reducing the number of buildings equal to the amount closed during each lockdown. The dates for each lockdown were days 90-150 for the first, days 300-330 for the second and days 360-420 for the third.

### 2.4 Calibration

The accuracy of the underlying model can be validated by removing all policies and only having one strain active. The mean initial reproductive rate,  $R_0$  of the virus, can then be measured to adjust the number of steps for each random walk and the duration of contact at each step.

In a paper by [Thye et al. \(2021\)](#), they analysed the transmissibility of different strains of COVID-19 and found that the average number of people that a contagious person will infect ( $R_0$  value) for the ancestral strain was 2.79. At the same time, the Delta variant had an  $R_0$  value of 5.08. Therefore, the model will first try to replicate the ancestral strain's  $R_0$  value. The initial number of infected people was set to 10 people as this makes sure that the chance that the virus dies out at the beginning is unlikely.

One crucial factor to consider is the natural immunity developed after someone has contracted a disease. A paper by [Hall et al. \(2022\)](#) found that the efficacy of natural immunity was around 86%; however, after one year, this dropped to 69%. Over a year, a simple linear decrease in efficacy will be used.

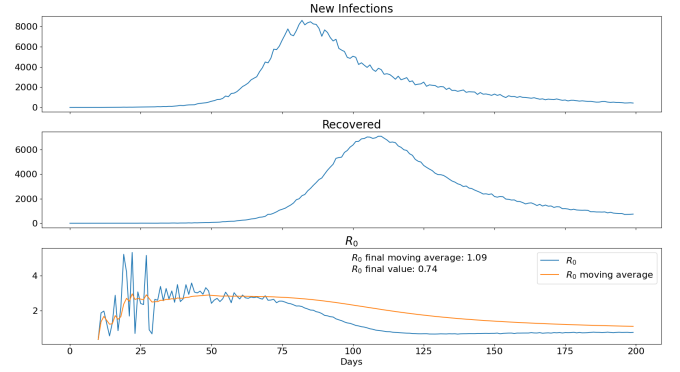


**Figure 7.** Initial infections due to ancestral strain of COVID-19 to calculate the initial reproductive value ( $R_0$ ).

The performance of the model can be modified by adjusting two variables. The first is the number of steps during the random walk in each building, and the second is the duration of contact from equation 2. The evolution of the unhindered COVID-19 can be seen in figure 7 where the parameters used were 50 steps per random walk and a contact duration of 0.5 seconds. After running the simulation, the model achieved the target reproductive value of  $R_0 = 2.79 \pm 0.31$  during the peak of the infection rate between day 30 and day 80. The peak infection rate is when  $R_0$  is the most stable, and there are no limitations to its spread.

If there is no change in conditions, a point of equilibrium will be reached, corresponding to an  $R_t$  value of one. Equilibrium occurs because as the number of new infections increases, there is a rapidly decreasing number of uninfected people; therefore, the infection rate must decrease as there are fewer interactions between infected and uninfected people.  $R_t = 1$  would correspond to one new infection per infected person, so there would be no overall change in the number of infected people.

The process can be repeated for the Alpha and Delta variants to produce values of  $\tau = 2$  and  $\tau = 3$ , respectively.

## 3 RESULTS

To test the model in several scenarios, first, the baseline will be taken to measure the spread of COVID-19 and its different variants without any precautions. The baseline will be compared to the different policies to measure their effectiveness. The simulation can then be run with one policy at a time to measure each policy's effect individually.

### 3.1 Baseline

The free spread of COVID-19 can be seen in figure 8. The first peak occurs on day 103, which corresponds to mid-April and reaches a maximum of  $7,095 \pm 128$  new cases per day.

After this peak, the number of new cases rapidly decreases and, as can be seen from figure 8(c),  $R_t$  falls to  $0.688 \pm 0.002$ , which will result in a higher recovery rate than the infection rate. However, as the number of people recovered increases, the reproductive rate increases linearly as it tends towards an equilibrium where  $R_t = 1$ . The number of new cases reaches a minimum of  $321 \pm 6$  new cases per day on day 269, just before the Alpha variant has come into effect. A true equilibrium is never reached for the ancestral strain as



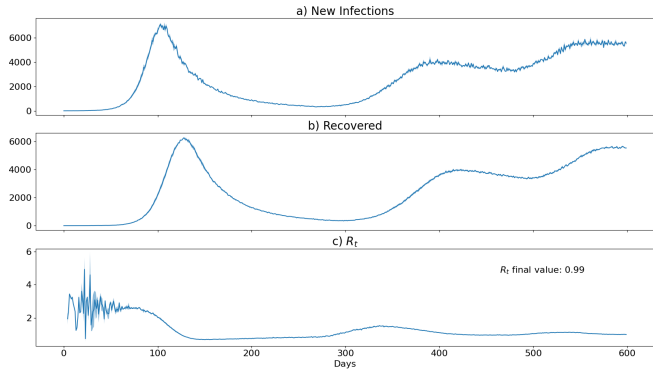


**Figure 8.** Spread of COVID-19 with each peak corresponding to each strain. (a) shows the number of new infections per day, (b) shows the number of people recovered per day and (c) shows the effective reproductive value over time which is found after someone has recovered.

$R_t$  reaches a maximum value of  $R_t = 0.825 \pm 0.011$  before the new variant comes into effect.

By day 330, the Alpha variant becomes the dominant strain, and  $R_t$  reaches a maximum of  $1.53 \pm 0.01$ . Shortly after this, the number of new cases rises to a maximum of  $4,213 \pm 109$  per day on day 398. However, due to the short time between the Alpha and Delta variant,  $R_t$  does not reach equilibrium.

On day 480, the Delta variant is starting to spread, and by 540, it has become the dominant strain. It can be seen in the graph that as  $R_t$  rises to  $1.139 \pm 0.002$  on day 532, the number of new infections increases to a maximum of  $5,863 \pm 74$  cases per day on day 555. Shortly after this, the model reaches its first equilibrium where  $R_t = 1$  and the recovery rate is equal to the infection rate of  $5,542 \pm 79$  people per day.

The recovery rate can be compared to the infection rate by taking the time of the first peak on each graph. The peak infection rate occurred on day 103, while the peak recovery rate occurred on day 128, leading to a 25 day lag between the two. The peak of the Alpha variant shows a similar lag of 25 days.

The total number of infections, including reinfections, came to  $1,567 \times 10^3 \pm 2 \times 10^3$  over the 600 days.

### 3.2 Testing

Figure 9 shows the model with testing in acted. The characteristics of the first peak up to the maximum for the ancestral variant are identical as testing has not yet come into effect. After the initial wave, the model with testing reaches a minimum of  $285 \pm 6$  new cases per day on day 271, 89% of the baseline.

During the peak of the Alpha variant, the maximum number of new infections reached  $4,036 \pm 43$  per day, 96% of the baseline, on day 422, 24 days after the baseline.

By day 485, testing has reached the maximum percentage of 3%. The maximum number of tests can be found at the midpoint between the peak number of Alpha cases and the maximum testing percentage. This number reaches  $311 \pm 8$  positive tests per day on day 432.

After the Delta variant has become the dominant strain, the number of new infections rises to a maximum of  $5,803 \pm 99$  new infections on day 575, 99% of the baseline.

During the Delta variant, the number of positive tests reaches a global maximum of  $520 \pm 12$  per day on day 577. The number of people isolating closely follows the number of positive tests; however,

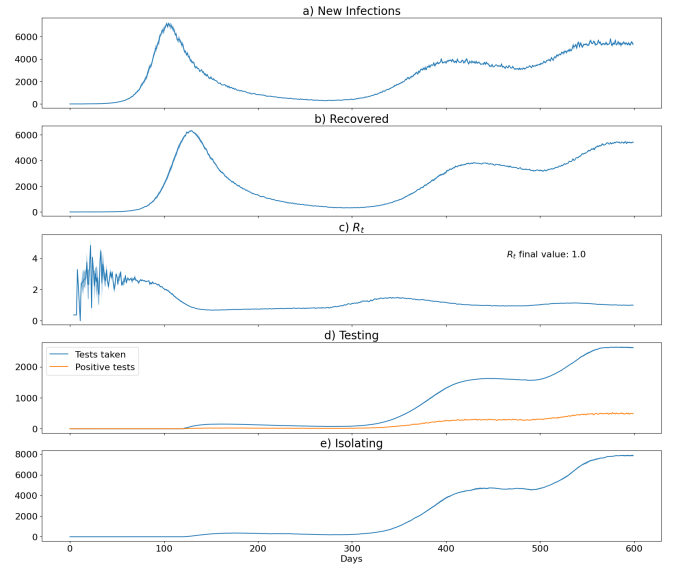


**Figure 9.** Spread of COVID-19 with testing enacted to reduce the spread. (a) shows new infections per day, (b) shows the number of people recovered per day, (c) shows the effective reproductive value  $R_t$ , (d) the number of tests taken by infected people per day as well as the number of positive tests and (e) shows the total number of people isolating each day.

with a slight lag as seen by the maximum of  $7,882 \pm 38$  on day 586 trailing the maximum for positive tests by 9 days and the maximum for new infections by 11 days.

After the Delta variant's peak, the number of new infections and the number of people recovering per day settles into an equilibrium of  $5,391 \pm 80$ , 97% of the baseline.

The total number of infections, including reinfections, came to  $1,500 \times 10^3 \pm 2 \times 10^3$  and the total number of times someone went into isolation was  $1,292 \times 10^3 \pm 1 \times 10^3$  over the 600 days. The average test success rate was  $18\% \pm 3\%$ .

### 3.3 Vaccinations

The effect of vaccinations can be seen in figure 10. Due to the late deployment of vaccinations, their effect starts to show during the Alpha variant, with the full effect only seen when the Delta variant is dominant.

The minimum number of new infections per day is comparable to the baseline of  $317 \pm 9$  on day 270, and only 1.7% of the population will have had their first dose.

After the Alpha variant has become dominant,  $R_t$  rises to a maximum of  $1.50 \pm 0.03$  on day 339. The number of new cases follows to a maximum of  $3,864 \pm 113$  on day 386, 92% of the baseline and 12 days earlier. At this time, 17% of the population will have had their first dose, and 1.6% will have had their second.

Unlike the baseline model, the number of cases for the Delta variant does not surpass the number of cases for the Alpha variant. On day 536,  $R_t$  gets to a maximum value of  $1.044 \pm 0.004$ . The maximum number of new infections was  $2,939 \pm 78$  on day 544, 50% of the baseline, and 11 days earlier. At this peak, 67% of people will have had their first dose, and 50% will have had their second vaccination.

Finally, an equilibrium is reached within the model's last few days with an equal infection rate and recovery rate of  $1,016 \pm 15$  per day. 76% and 72% have at least one dose and two doses, respectively, by the end of the simulation.

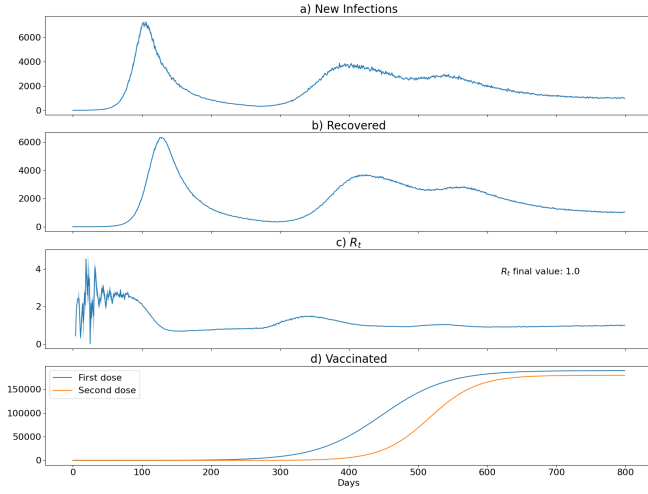


**Figure 10.** Spread of COVID-19 with vaccines arriving towards the end of the period. (a) shows new infections per day, (b) shows the number of recoveries per day, the effective reproductive value,  $R_t$ , and (d) the current number of vaccinations for both one dose (blue) and two doses (orange).

The total number of infections, including reinfections, summed to  $1,244 \times 10^3 \pm 2 \times 10^3$  over 600 days and  $1,500 \times 10^3 \pm 2 \times 10^3$  over the 800 days.

### 3.4 Social distancing

Figure 11 shows what the effect of imposing social distancing throughout the pandemic would do. After day 60, social distancing starts, which can be seen in the sudden drop of  $343 \pm 25$  new cases per day on day 59 and  $152 \pm 13$  cases per day on day 60. Compared to the baseline, the initial peak shows an immediate difference as it spreads out until the Alpha variant becomes dominant. A peak number of new infections per day occurs on day 162, 59 days later than the baseline, and only reaching a maximum of  $872 \pm 65$  new cases per day, 12% of the baseline.

On day 292, a minimum is reached before the Alpha variant becomes dominant. The minimum occurs 23 days before the baseline with a minimum of  $146 \pm 24$  cases per day, 175 cases below the baseline.

When the Alpha variant becomes the dominant strain and causes the second wave, a maximum of  $965 \pm 56$  new cases, 23% of the baseline, occurs on day 434, 36 days after the baseline.

Finally, when the Delta variant becomes the dominant strain, a maximum of  $1,379 \pm 192$  is reached on day 598, 24% of the baseline. The maximum occurs 43 days after the baseline.

An equilibrium is approached towards the end of the model of  $451 \pm 3$  new cases and recoveries per day.

The total number of COVID-19 cases, when summed over the first 600 days, reaches  $347 \times 10^3 \pm 2 \times 10^3$ , 22% of the baseline, and when summed over the whole period, the total number of cases is  $585 \times 10^3 \pm 2 \times 10^3$ .

### 3.5 Lockdowns

The spread of COVID-19 with the policy of lockdowns can be seen in figure 12.

After day 90, the first lockdown begins. The number of cases just before the lockdown was at  $4,586 \pm 384$  and dropped to  $3,737 \pm 308$

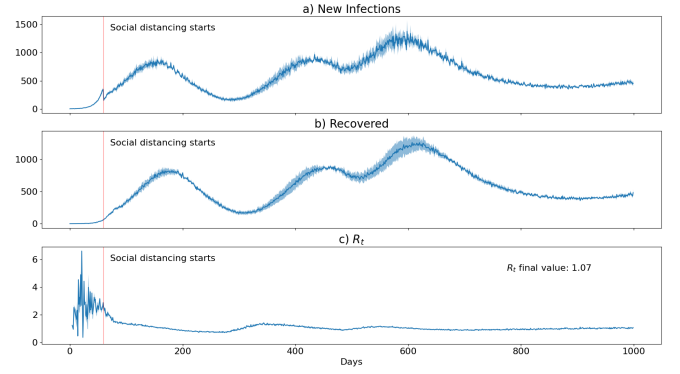


**Figure 11.** Spread of COVID-19 with social distancing enacted after the read line on day 60. (a) shows new infections per day, (b) shows number of recoveries per day and (c) shows the effective reproductive value  $R_t$ .

when the lockdown began. The lockdown period lasted throughout the peak of the first wave resulting in the maximum number of new infections per day, reaching  $5,395 \pm 82$  on day 103, 76% of the baseline.

During the first lockdown, the effective reproductive value goes as low as  $0.626 \pm 0.008$  on day 141.

After day 150, the first lockdown ended with cases reaching a minimum of  $584 \pm 13$  on day 271, 182% of the baseline.

On day 300, the second lockdown begins and lasts for 30 days; this occurs just before the Alpha variant becomes dominant but before the peak. The third lockdown then follows this on day 360, which lasts 60 days throughout the peak of the Alpha variant. The maximum number of new infections during this period is  $3,677 \pm 52$ , 87% of the baseline on day 357, 41 days before the baseline and lies in the period between the two lockdowns. During the lockdowns, the maximum number of cases per day reaches  $3,402 \pm 59$  on day 373, which is only 25 days behind the baseline and during the third lockdown.

As the final lockdown ends on day 420 and the Delta variant starts on day 480, the lockdowns will have no direct effect on the peak for the Delta variant. The maximum is slightly higher than the baseline as it reaches  $6,005 \pm 478$  on day 558, 102% of baseline; however, this is within uncertainty. The model then settles into an equilibrium of  $5,581 \pm 24$ .

Overall, the total number of infections reaches  $1,540 \times 10^3 \pm 3 \times 10^3$ , 98% of the baseline.

## 4 DISCUSSION

The effects of the different methods to control the spread of COVID-19 can be evaluated by comparing them to the model with no precautions. There are some inaccuracies that all models rely on, such as:

- the distribution of building properties follow Gaussian distributions
- the number of people visiting a building per day and the number of buildings visited by a person per day
- no correlation between people visiting a building and the next building
- movement of people with no intelligence, as they walk due to random numbers

Finally, another problem is the problem of trying to model a complex environment with many variables, which means that while any-

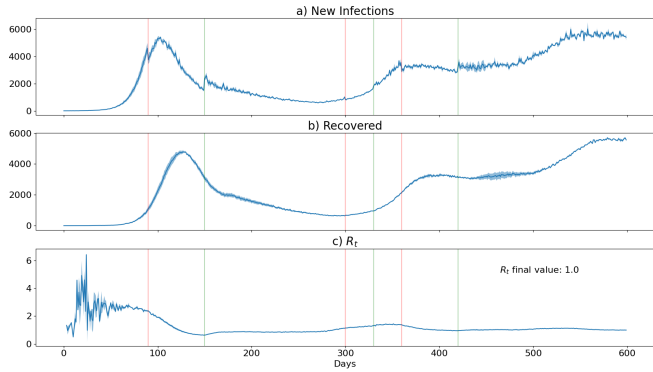


**Figure 12.** Spread of COVID-19 with lockdowns enacted. Red signifies the start of a lockdown and green signifies the end. (a) shows new infections per day, (b) shows number of recoveries per day and (c) shows the effective reproductive value  $R_t$ .

one variable may have a negligible effect on the model, the combination of many of these small variables can add up to result in significant inaccuracy.

While the models try to be accurate, their numbers cannot necessarily be taken at face value. While one model may appear to have a much more significant impact on the spread of COVID-19 compared to another, these numbers could quickly change when applied to reality. The primary purpose would be to assess how each policy affects the spread by changing the distribution of daily infections and the other recorded data. It can also give an idea of how well the UK government's policies worked in their timings for when they were enacted and to the level of their implementation. However, while the methods may appear to only show benefits in reducing the spread of COVID-19, this conclusion does not consider the cost of these policies either economically, mentally or otherwise. It also does not take into account development times. Some of this can be seen in the models, such as development times for testing and vaccinations.

#### 4.1 Testing

As seen in section 3.2, at the current testing rate of 3%, this policy only has a slight impact on the reduction in infections, with the maximums of each wave only getting reduced by a few per cent, with the most significant difference during the peak of the Alpha wave with a reduction in 177 cases per day. There is also no change in the peak of the ancestral variant due to the delayed roll-out of testing.

Most of the differences were within one or two standard deviations. Therefore, there is no significant difference between the two methods. The slightest difference is during the maximum of the Delta wave, with only a difference of 60 new cases per day.

As can be seen from both figure 8 and figure 9, testing does not have a significant effect on the rate of spread of COVID-19 over time. A similarity between the models can be seen in the over-saturation during the Delta variant. This over-saturation suggests that the number of uninfected people is limiting the spread of the virus.

However, the reduction in cases each day does add up throughout COVID-19, summing to a total reduction of 67,000 infections or 4% of the total number of infections and several times the standard deviation, marking a clear impact that testing has on the reduction of cases and reducing the impact of COVID-19.

This result means that for a testing rate of 3%, with some bias towards symptomatic testing, a 4% reduction of cases is observed,

suggesting that more selective testing techniques and higher testing percentages will result in a more significant reduction in the number of infections.

However, several assumptions and approximations were made in this model, resulting in lower accuracy. It is hard to know why people take tests; there will be a significant difference if tests are more targeted than the binary options used in this model. Some improvements could be to account for people taking tests who were in contact with someone who recently tested positive for COVID-19, and people who go out more or are going to a big event would test more frequently. This model only accounts for PCR and lateral flow tests and not any other forms of testing such as antibody testing.

While the testing policy does not dramatically reduce the spread of COVID-19, at a testing rate of only 3%, there is a noticeable reduction in the number of people who will get infected.

#### 4.2 Vaccinations

The results for the policy with vaccinations enacted can be seen in section 3.3. Due to the delay in rolling out the vaccinations, there is no difference in the peak of the ancestral variant and the period between the first two variants. While the minimum is slightly lower with vaccinations than the baseline, both results are within the uncertainty of each other.

However, as the number of vaccinated people increases, vaccines' effect can be seen by reducing the number of new infections for both the Alpha variant and the peak of the Delta variant. Unlike the previous simulations, the peak of the Delta variant is lower than the peak for the Alpha variant. The lower peak is due to the higher number of vaccinated people, especially people with a second dose. There were only 1.6% with a second dose during the Alpha strain, which increased to 50% during the Delta variant. The number of people with the first dose also significantly increased from 17% to 67%.

Even with a negligible number of people with a second dose and only 17% with the first, the simulation with vaccinations achieved a reduction of 8% of new cases per day at the peak of the Alpha variant; however, the difference is only a couple of standard deviations, so the result is not strongly independent.

However, after the Delta variant reaches its maximum, there is a significant reduction in cases per day. In the vaccination model, the peak number was 50% less than the baseline, a significant difference compared to the standard deviation of each result.

Another interesting result was that the peak for the Alpha and Delta variant was reached earlier than for the baseline. Both results had roughly the same difference of 12 days and 11 days, respectively. This difference is likely due to a maximum value for  $R_t$  that each variant can achieve in different scenarios. Due to the increased resistance of people with vaccinations, this value was smaller, with the Delta variant seeing the most significant difference. However, the Alpha variant was within the uncertainty of the baseline. Another difference was that the maximum for  $R_t$  was achieved later than the baseline, suggesting a smoothing out of the reproductive rate for the model with vaccinations, resulting in a lower maximum of new cases and a more uniform distribution.

A 21% reduction in the total number of cases during the same period shows the advantages of vaccinations.

However, the efficacy of vaccinations over time was not considered for this model. As the time since getting the vaccination increases, the efficacy of the vaccination is likely to decrease due to mutations in different variants as the properties of the vaccine become more different to the new viruses. However, there was conflicting evidence



on whether or not the vaccine efficacy was reduced due to the Delta variant. There also was evidence found to suggest a reduction in vaccine efficacy for the Alpha variant; therefore, the vaccine efficacy was kept constant throughout the model. Another consideration to improve the model's accuracy would be to account for the short period after getting the vaccination. The immune system builds up its protection during this period, resulting in a delay before maximum protection. As this model only simulates the first three variants of COVID-19, vaccine boosters were not simulated. The goal of a booster is to add further protection against the different variants and counter any decrease in efficacy that the current vaccines may have experienced over time. Booster vaccinations would have started around day 600. Another simplification was that the protection of an individual is given by whichever source gives the most protection individually. Therefore, the additional protection of previously having COVID-19 and a vaccination was not considered.

Overall, vaccinations have shown a clear benefit in reducing the spread of COVID-19 throughout the simulation; however, these alone have shown that they cannot eliminate the spread of COVID-19.

### 4.3 Social Distancing

Section 3.4 shows that the early roll-out of social distancing has an immediate effect by the sudden reduction in the number of cases by 191 per day, which is significant compared to the standard deviations of the uncertainty providing evidence for the benefit of social distancing.

The effect of social distancing can be further seen in the significant reduction of 88% of cases during the ancestral variant for COVID-19. This reduction is not seen in the previous two models due to their late start date, which gives social distancing an advantage over the other methods.

Further reductions can be seen in the peaks for the Alpha and Delta variants with reductions of 77% and 76%, respectively. These reductions show that the spread of COVID-19 among people is incredibly sensitive to the separation distance.

Another advantage can be seen in the width of each peak, with several days of delay between the two models. The delay varies from 36 days after the baseline to 59 days later, which would significantly help with problems faced by the overloading of medical facilities.

One difference in this model is the more significant uncertainty in the results than the others. This uncertainty suggests that the underlying randomness affects the model to a greater degree, especially in the rise to each maximum.

However, this model will have inaccuracies in modelling the average number of people maintaining social distancing and the periods when this is more enforced versus the periods where guidelines are loosened. The model assumes that as soon as the introduction of the first social distancing guidelines, this was kept constant. However, the model accounts for some variability in the separation between people and densities larger than the social distancing densities.

Overall, social distancing has clearly shown that, if properly enacted, it can drastically reduce the spread of COVID-19.

### 4.4 Lockdowns

As seen in section 3.5, lockdowns are shown to help reduce the maximum number of daily infections during each period that they were enacted. Like social distancing, lockdowns benefit from being brought out early in the spread of COVID-19 and therefore target the initial spread of the ancestral variant. However, lockdowns also

ended the earliest of all the models and therefore had little effect when the Delta variant became the dominant strain.

Reductions in the maxima of the ancestral and Alpha variants were 24% and 13% respectively; however, only a marginal 2% reduction was seen in the total number of infections. The explanation for the slight reduction in cases can be seen from the minima in the simulation, with the minimum after the ancestral variant being 1.82 times more than the baseline. The physical explanation is likely due to the reduced number of people with natural immunity as fewer people got infected during the first peak. Therefore, lockdowns appear to act more to spread out the number of infections rather than reduce the total number. However, later in the model, this difference is less noticeable. The only other time it can be seen is after the Delta variant by comparing the number of daily infections at equilibrium, where the difference between the two models is within uncertainty. This negligible difference could be due to no lockdowns during the peak of the Delta variant, or it could be due to a large number of people who already have natural immunity.

However, this model will have some inaccuracies due to approximations and simplifications. One assumption is that everything is immediately brought back to normal after each of the three lockdowns. However, in the UK, there were varying levels of restrictions enacted throughout the different stages of the spread of COVID-19, which would help to further reduce the spread of COVID-19 during the period where no lockdowns were enacted. Another assumption is that the percentage of businesses closed during a lockdown did not affect the properties of each building which would be an unrealistic assumption. Many buildings that would be shut down would be entertainment facilities which would likely be places of greater spread of COVID-19. In contrast, places that remain open are likely operating at reduced capacity and would therefore be less likely to spread COVID-19 between people.

Overall, while lockdowns have a negligible effect on the total number of people contracting COVID-19, they help reduce the demand on medical facilities by spreading the infections over more extended periods.

## 5 CONCLUSIONS

This paper aimed to access different methods that the UK government used to try and reduce the spread of COVID-19.

Due to the many variables and complexities that affect virus propagation and the different policies, many assumptions and simplifications had to be made, resulting in simulation inaccuracies. Therefore, each model shows how an individual policy can affect the spread of COVID-19 and its unique effects rather than directly comparing the exact numbers between different models.

It was found that each model would affect the spread of COVID-19 in different ways. Testing provided a percentage reduction throughout the period that it was active; however, it has little effect on the ancestral variant due to its late start. Vaccinations were found to reduce cases significantly; however, they had a much slower build-up, so the full extent was only seen during the final stage of the model when the Delta variant was the dominant strain. Social distancing was shown to spread and reduce the number of infections while also being enacted early in COVID-19. Finally, lockdowns had the effect of spreading out the number of infections rather than directly reducing them, which would be beneficial in reducing the load on medical facilities.

Therefore, this information can help build upon the research to

understand how different policies can affect the spread of COVID-19 and help prevent future outbreaks from becoming pandemics.

## REFERENCES

- Alene M., Yismaw L., Assemie M. A., Ketema D. B., Mengist B., Kassie B., Birhan T. Y., 2021, PLoS one, 16, e0249090
- Bale R., Iida A., Yamakawa M., Li C., Tsubokura M., 2021, arXiv preprint arXiv:2110.04295
- Borchert J. G., 1998, GeoJournal, 45, 327
- Byrne A. W., et al., 2020, BMJ open, 10, e039856
- Chandra S., Bharti A. K., 2013, Procedia-Social and Behavioral Sciences, 104, 660
- Chaslot G., Bakkes S., Szita I., Spronck P., 2008, in Proceedings of the AAAI Conference on Artificial Intelligence and Interactive Digital Entertainment. pp 216–217
- Fang Z., Lo S., Lu J., 2003, Fire Safety Journal, 38, 271
- Gautret P., et al., 2020, Expert review of clinical immunology, 16, 1159
- Hall V., et al., 2022, New England Journal of Medicine
- Hanrahan P., 2010, Monte Carlo Path Tracing
- Heath P. T., et al., 2021, MedRxiv, pp 2021–05
- Hendaus M. A., Jomha F. A., 2021, Qatar Medical Journal, 2021, 49
- Jensen H. W., Arvo J., Dutre P., Keller A., Owen A., Pharr M., Shirley P., 2003, in ACM SIGGRAPH.
- McAloon C., et al., 2020, BMJ open, 10, e039652
- Mohamed S., Rosca M., Fignunov M., Mniha A., 2020, J. Mach. Learn. Res., 21, 1
- Montanaro A., 2015, Proceedings of the Royal Society A: Mathematical, Physical and Engineering Sciences, 471, 20150301
- NumPy 2022, Random Generator, <https://numpy.org/doc/stable/reference/random/generator.html#:~:text=It%20uses%20Mersenne%20Twister%2C%20and,probability%20distributions%20to%20choose%20from.>
- Parliament U., 2021, Coronavirus: A history of English lockdown laws, <https://commonslibrary.parliament.uk/research-briefings/cbp-9068/>
- Polack F. P., et al., 2020, New England Journal of Medicine
- Pouwels K. B., et al., 2021, Nature medicine, 27, 2127
- Predtechenskii Vitaly M. A. I. M., 1978, Planning for foot traffic flow in buildings. National Bureau of Standards, US Department of Commerce, and the National ...
- Rickman H., Wiśniowski T., Wajer P., Gabrysowski R., Valsecchi G., 2014, Astronomy & Astrophysics, 569, A47
- Thye A. Y.-K., Loo K.-Y., Tan K. B. C., Lau J. M.-S., Letchumanan V., 2021, Progress In Microbes & Molecular Biology, 4
- ToolBox E., 2003, Required Space per Person, [https://www.engineeringtoolbox.com/number-persons-buildings-d\\_118.html](https://www.engineeringtoolbox.com/number-persons-buildings-d_118.html)
- UK government 2020, reasons for getting a covid-19 test: survey of regional and local testing sites between 1 and 4 september, <https://www.gov.uk/government/publications/survey-reasons-for-getting-a-coronavirus-covid-19-test-reasons-for-getting-a-covid-19-test-survey-of-regional-and-local-testing-sites-between-1-and-4-september>
- UK government 2021, HM Government Social Distancing Review, [https://assets.publishing.service.gov.uk/government/uploads/system/uploads/attachment\\_data/file/999413/Social-Distancing-Review-Report.pdf](https://assets.publishing.service.gov.uk/government/uploads/system/uploads/attachment_data/file/999413/Social-Distancing-Review-Report.pdf)
- UK government 2022b, Coronavirus and behaviour of the vaccinated population after being in contact with a positive case in England - office for national statistics, <https://www.ons.gov.uk/peoplepopulationandcommunity/healthandsocialcare/healthandwellbeing/bulletins/coronavirusandbehaviourofthevaccinatedpopulationafterbeingincontactwithapositivecaseinengland/10januaryto15january2022>
- UK government 2022a, Testing in United Kingdom, <https://coronavirus.data.gov.uk/details/testing>
- Wikipedia 2022a, Markov chain, [https://en.wikipedia.org/wiki/Markov\\_chain](https://en.wikipedia.org/wiki/Markov_chain)
- Wikipedia 2022c, Monte Carlo method, [https://en.wikipedia.org/wiki/Monte\\_Carlo\\_method](https://en.wikipedia.org/wiki/Monte_Carlo_method)
- Wikipedia 2022b, Random walk - Wikipedia, [https://en.wikipedia.org/wiki/Random\\_walk](https://en.wikipedia.org/wiki/Random_walk)
- for National Statistics O., 2021, Coronavirus: how people and businesses have adapted to lockdowns, <https://www.ons.gov.uk/economy/economicoutputandproductivity/output/articles/coronavirushowpeopleandbusinesseshaveadaptedtolockdowns/2021-03-19>

## APPENDIX A: RANDOM WALK AND RANDOM NUMBERS

Random walk, as explained in section 2.2, uses a random number generator to create a random walk. As the model was made using Python, the library NumPy was used to generate random numbers. NumPy uses the pseudo-random number generator based on Mersenne Twister (NumPy 2022). The advantage of the Mersenne Twister is that it can generate pseudo-random numbers with a substantial period of  $2^{19937} - 1$ ; it has passed several tests in determining the quality of randomness and can generate random numbers very quickly. However, one major problem is that it is deterministic, so it is not cryptographically secure, and it does not pass all randomness tests.

The foundation of a random walk is that each step only depends upon the previous step, and each possible path has an equal probability. This independent process means that a random walk follows a Markov process (Wikipedia 2022a). A straightforward implementation is a random lattice walk where a point can move in a 2D plane; however, it can only move with perpendicular vectors resulting in grid movement with each step size equal (Wikipedia 2022b). This basic model can be expanded to include higher dimensions, more complex movement, including varying step sizes, freedom to move in any direction and different probability distributions for random number generations.

## APPENDIX B: MONTE CARLO SIMULATIONS

Monte Carlo simulations take advantage of the law of large numbers, where results generated from randomness will converge on the true answer as the number of data points increases. In general, Monte Carlo simulations can be broken up into four main steps (Wikipedia 2022c). The first is to determine the probability distribution(s) that the data will be drawn from, generate large amounts of input data, pass the data into a deterministic algorithm, and finally, process the result to get an analytical answer. The simulation used in this paper uses Monte Carlo simulations when calculating the number of people infected each day. In addition, the repeated runs for each model also act as a miniature version of a Monte Carlo simulation. The Monte Carlo simulation first defines probability distributions to describe different properties of buildings and the number of infected people. Then, environments are created using these probability distributions. The created environments are then passed into the random walk, which calculates the number of infections per building. Finally, this number can be returned to process the total number of new infections and passed into the program.

The advantages of Monte Carlo simulations are that they are easy

to set up, take in a range of inputs, and simulate the chaotic nature of systems. However, Monte Carlo simulations can be very inefficient and time-consuming, and if the inputs are not fully defined, the outputs might not return accurate results.

## APPENDIX C: USES IN PHYSICS

Due to the general nature of Monte Carlo simulations, they have many applications both within physics and outside of physics. Although not a direct application, a paper by [Montanaro \(2015\)](#) used quantum computers to provide quadratic speedup over classical computers when calculating Monte Carlo simulations, in particular, partition functions. Quantum Monte Carlo simulations can be created by taking advantage of the reversible nature of quantum circuits and quantum amplitude amplification to obtain higher probabilities for the desired answer that can be achieved on a classical computer. This paper proposed several applications for this method. One was to simulate the Ising model for ferromagnets, where the lowest energy state for the spins of atoms within the lattice can be found above the critical temperature. Using the Gibbs distribution and Glauber dynamics to create the initial mixing of states and the system's evolution, it was found that the quantum Monte Carlo simulation approximates the answer within a relative error faster than a classical algorithm as the errors are reduced.

In a paper by [Rickman et al. \(2014\)](#), they investigated the use of several different Monte Carlo simulation methods in predicting the probability of impact events for a given planet, with the singularities in the equations being of particular interest which have previously caused problems. They then used numerical methods to test the performance of the models and found that all models were in close agreement with each other. The models also proved to be efficient in terms of computational time.

## APPENDIX D: USES OUTSIDE OF PHYSICS

Monte Carlo simulations also have many applications outside of physics. One application is in computer graphics to generate rays for accurate lighting effects. The basics of ray tracing are to project rays from the pixels of a virtual camera and follow the path, calculating any reflection, refractions and diffusions when the ray meets a surface. Alternatively, rays can be calculated from light sources and traced back to the camera. The general algorithm follows: randomly sample a ray from the camera, trace the ray until it intersects with a surface, determine if the surface is an emission surface or reflective surface, if emission, then terminates as this is a light source; otherwise, randomly scatter the ray according to the surface and repeat the process until it reaches an emission source ([Hanrahan 2010](#)). This process can be seen as a Monte Carlo simulation as large numbers of rays are generated with random properties. They are then emitted, and calculations are performed to determine the view properties of surfaces that intersect, and this data is returned to generate the final image. The advantages of Monte Carlo simulations for ray tracing are that it does not require as much memory, graphics do not need to be precomputed, reduce sharp lines due to randomness, and are very easy to implement. However, Monte Carlo simulations in ray tracing can be slow, and they suffer from noise due to the variance in the rays. The amount of noise is sample dependent, so the more rays, the less noise; however, the greater the performance cost ([Jensen et al. 2003](#)).

Another use for Monte Carlo simulations is in game AI using tree

search to find the best moves to win the game. The aim is to build a tree of optimal moves so that when the program encounters one branch of the tree, it will know which move is best. Weights can be learned and applied to each branch, and the chosen path will be randomly chosen with probabilities depending upon the weights. The tree can be built by first choosing a state that already exists in the tree. The program will follow the branches of existing states depending on two factors; the first is exploitation, where the goal is to get the best result, and the second is an exploration, where the goal is to try out less promising paths to try and reduce biases. The program will try out each state down a branch until it reaches a point where there are no more states. It can now create a new node. At this point, the program will play the rest of the game, making random moves until the game ends. The last step is to calculate backpropagation which assigns weights to each path depending on the win/loss ratio. When the program is applied to a real game, it will choose the actions that lead to states that were visited the most. This technique has been implemented in many different scenarios, from board games to real-time strategy games and can create programs that have won GO competitions ([Chaslot et al. 2008](#)).

Like the previous application, Monte Carlo simulations can be used for gradient estimation in machine learning programs, as found in a paper by [Mohamed et al. \(2020\)](#). Machine learning can be simplified to be considered an optimisation problem. The goal is to find the best weights for each node in the network that leads to the highest accuracy in predictions when given an input. This is done using gradient descent methods where the gradient in hyper-parameter space is calculated, and the weights are adjusted to follow the direction of a decreasing function. However, Monte Carlo simulations can speed up pathwise gradient calculations to estimate the gradient of the cost function. The reason for choosing Monte Carlo estimation over numerically calculating the gradients is that due to many parameters, it can be difficult and inefficient to use alternate methods such as quadrature for integration, or the function might not be differentiable. Monte Carlo simulations can be used by sampling several paths and transforming them using a deterministic path; the cost function can be calculated.

This paper has been typeset from a  $\text{\LaTeX}$  file prepared by the author.